Mechanism of particle removal by megasonic waves

Wonjung Kim,[1] Tae-Hong Kim,[1] Jaehyuck Choi,[2] and Ho-Young Kim[1,a)]
[1]*School of Mechanical and Aerospace Engineering, Seoul National University, Seoul 151-744, Republic of Korea*
[2]*Semiconductor Business, Samsung Electronics, Yongin, Gyeonggi 449-711, Republic of Korea*

(Received 23 October 2008; accepted 6 February 2009; published online 26 February 2009)

We elucidate the major mechanism of microparticle removal in the megasonic cleaning process through the direct visualization experiments. It is revealed that particles sitting on solids are removed by adjacent microbubbles that oscillate near the substrates and exert interfacial and pressure gradient forces on the particles. Other pressure and streaming effects are shown to be too weak to detach the particles. © *2009 American Institute of Physics*. [DOI: 10.1063/1.3089820]

Ultrasonic cleaning processes, which use frequencies of the order of 10^6 Hz, are called the megasonic cleaning and widely employed for cleaning of photomasks and wafers in semiconductor industries and of ceramic membranes in environmental industries.[1] In liquid under megasonic waves, various fluid dynamic phenomena occur: pressure gradients are formed,[2] acoustic streaming flows are generated,[3] and microcavitation bubbles oscillate and dance around due to Bjerknes force.[4] Despite well-established observations of these flow behaviors and of consequent cleaning of immersed surfaces, the physical explanation of how the particles are removed is still far from clear. Thus here we aim to elucidate the major mechanism of particle removal due to megasonic waves. A variety of forces has been proposed to be responsible for the particle removal thus far including the forces due to acoustic pressure gradient,[5] acoustic streaming,[6] and microcavitation.[1] Also chemical effects[7] are known to play a role when the cleaning is performed in chemical solutions such as a standard cleaning solution SC-1. Here we only focus on hydrodynamic effects induced by megasonic waves, which are often sufficiently effective to completely remove small particles.

Since the lack of understanding of the cleaning mechanism mainly comes from the extreme difficulty in observing the particle removal process, we construct a visualization apparatus for the megasonic cleaning. As shown in Fig. 1(a), the experimental setup consists of a quartz bath, on one of whose sides a piezoelectric transducer with the resonance frequency of 0.95 MHz is attached, an upright microscope (Olympus BX-51M) with a water immersion objective lens (Olympus LUMPLFL 100XW), and a high-speed camera (Photron APX-RS). As solid surfaces to be cleaned, we use the most common semiconductor material surfaces, i.e., bare Si wafers and Si wafers with micropatterns fabricated by an reactive ion etching process as shown in Fig. 1(b). In addition, Al surfaces were used since a few bubbles are observed to remain attached once in contact with the surfaces (although very rare) probably due to their enhanced hydrophobicity (the static contact angle of water on Si and Al being 40° and 55°, respectively), while no such sitting bubbles are seen on flat Si surfaces. As contaminant particles, we use fluorescent spherical polystyrene latex (PSL) particles of two different diameters: 0.71 and 1 μm. Before cleaning, the particles are attached to a surface by an atomizer as mixed with isopropyl alcohol. Then we wait 3 h to regulate the adhesion force before immersing the wafer in de-ionized water. In addition to visualizing the flow, we measure the acoustic pressure provided by the transducer with a needle hydrophone (Precision Acoustics HPM02/1) having a sensor diameter of 200 μm.

To determine which mechanism is responsible for detaching particles from substrates, we first estimate the strength of adhesion between the particles and the substrates and compare its magnitude with detachment torque resulting from each proposed mechanism. The adhesion force of a micron- or submicron-sized particle to a solid surface is mainly due to the van der Waals force.[8] When a sphere is in contact with a flat surface, the van der Waals interaction force F_v is given by $F_v = \frac{1}{6}AR/Z_0^2$, where A is the Hamaker constant, R the particle radius, and Z_0 the distance between the particle and the flat surface normally taken to be approximately 0.4 nm.[9] Adding the effects of particle deformation as observed in Fig. 1(c), the total adhesion force F_a is given by $F_a = F_v(1 + a^2/RZ_0)$, where $A = 2.08 \times 10^{-20}$ J for a PSL par-

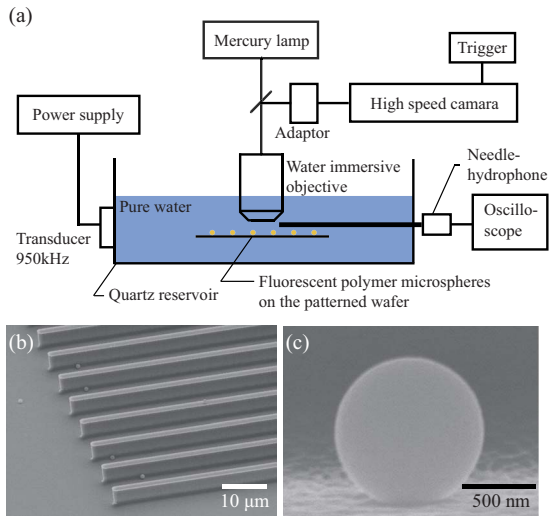

FIG. 1. (Color online) Preparations for visualization experiments. (a) Schematic of the apparatus. (b) Scanning electron microscopy (SEM) image of a Si wafer with line patterns on which contaminant particles have been deposited. (c) SEM image of a deformed particle on a silicon wafer after 3 h of contact.

a)Author to whom correspondence should be addressed. Electronic mail: hyk@snu.ac.kr.

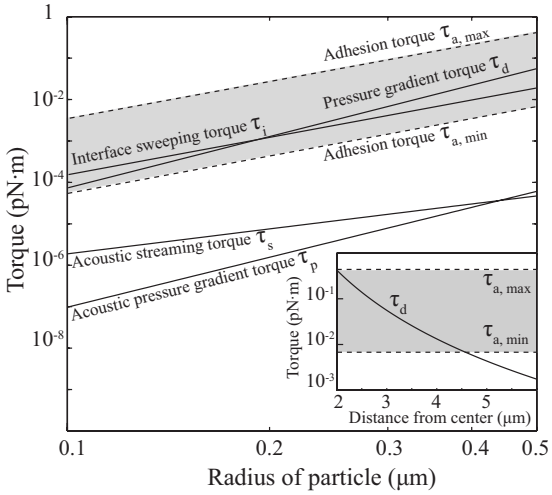

FIG. 2. Comparison of the scales of adhesion and detaching torques exerted on submicron-sized particles. The adhesion torque varies as the contact radius ranges from 0.1 times ($\tau_{a,\min}$) to 0.4 times ($\tau_{a,\max}$) the particle radius. Inset: decay of τ_d with the radial distance from the bubble center for the particle whose radius is 0.5 μm.

ticle on Si surface immersed in water and a is the particle-substrate contact radius.[8] The degree of particle deformation depends on the particle rigidity and the duration of contact. In Fig. 2, we plot the adhesion torque $\tau_a \sim aF_a$ of a spherical polymer particle on a silicon surface as a function of the particle radius.

When the wavelength of ultrasonic vibration is longer than the particle size, a force due to acoustic pressure gradient ∇p is exerted on the particle.[5] For a megasonic wave with the pressure amplitude A_p and the wavelength λ, $|\nabla p| \sim A_p/\lambda$. We write $A_p = \sqrt{2}p_m$ and $\lambda = 2\pi c/\omega$, where p_m is the root mean square of the pressure, c is the sound speed, and ω is the angular frequency. Multiplying $|\nabla p|$ with the particle volume and the moment arm ($\sim R$) gives the detachment torque due to acoustic pressure gradient $\tau_p \sim \omega p_m R^4/c$. The currently employed transducer generates $p_m = 260$ kPa as measured by the hydrophone. As shown in Fig. 2, τ_p is orders of magnitude weaker than the adhesion torque for submicron-sized particles, revealing the insufficient strength of the acoustic pressure gradient effect in megasonic cleaning.

Acoustic streaming that leads to nonzero time-averaged velocity of fluid under ultrasonic field is caused by decay and attenuation of sound field in viscous fluids.[3] Particles of our interest are of the similar size to the acoustic boundary layer whose thickness $\delta_{ac} \sim \sqrt{2\nu/\omega} = 0.58$ μm, where ν is the kinematic viscosity of water. Neglecting the effects of the wall (resulting in the upper bound of the force), the detachment torque τ_s by the drag force on spherical particles under low Reynolds number (Re) acoustic streaming flow is given by $\tau_s \sim 6\pi\mu u R^2$, where μ is the dynamic viscosity and u the acoustic streaming velocity. The maximum acoustic streaming velocity reaches 1 cm/s in our experimental apparatus as measured by particle image velocimetry, giving $\mathrm{Re} = R_u/\nu \sim 0.004$, which results in τ_s much lower than the adhesion torque as shown in Fig. 2.

Now that the scales of the torque induced by the acoustic pressure gradient and the acoustic streaming are shown to be orders of magnitude smaller than the adhesion torque of submicron-sized particles, it is natural to examine the effects

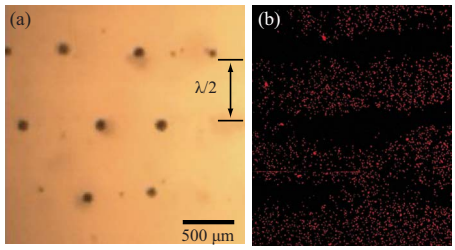

FIG. 3. (Color online) Effects of bubbles on surface cleaning. (a) Bubbles dancing in pressure nodes around a Si surface. (b) A micrograph of the cleaned surface showing that fluorescent particles have been removed only where bubbles were.

of bubbles on particle removal. The radius of the most active or resonant bubbles in an ultrasonic field is given by Minnaert's formula[2] $R_b = \sqrt{(3kP_0/\rho)}/\omega$, where k is the adiabatic exponent (~ 1.4 for mixture of oxygen and nitrogen, dominant gas contents in bubbles[10]), P_0 is the ambient pressure, and ρ is the liquid density. In our megasonic field, R_b is calculated to be approximately 3 μm, agreeing with the radius of the most active bubbles experimentally observed. In an experiment using a low acoustic pressure input ($p_m = 50$ kPa) from the transducer, we found that the particles were cleaned off only in the pressure nodes where the cavitation bubbles were confined (Fig. 3 and supplemental video available online[11]). With increased acoustic pressure input ($p_m = 260$ kPa), the bubbles moved around instead of being confined in the nodes (considered to be caused by enhanced acoustic streaming and complicated acoustic field due to an increased number of bubbles), thus cleaned the whole surface area. In addition, we observed that a single bubble left behind clean traces upon traveling on the particle-laden surface (see supplemental videos available online).[11] These provide direct evidences that bubbles play critical roles in megasonic cleaning, dominating other acoustic effects. In the following, we describe further visualization results elucidating how bubbles remove particles from solid surfaces.

Figure 4(a) shows microparticles being drawn to a bubble that translates on a wafer surface. The detached particles disappear from the subsequent images because they are levitated by microvortices circulating around the bubble[12]

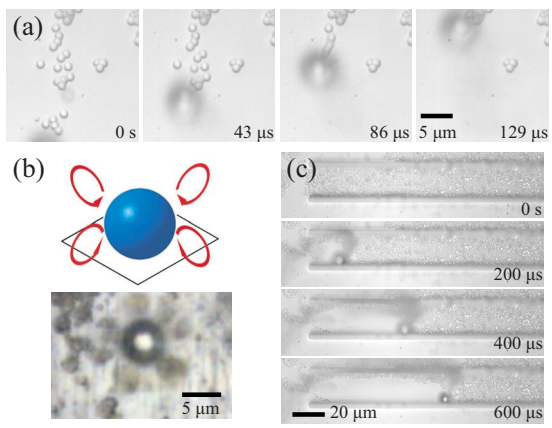

FIG. 4. (Color online) Particle motion induced by megasonic bubbles. (a) Detachment of particles on a flat Si wafer after 3 h of contact. Depth of focus of the objective lens is approximately 2 μm. (b) Circulation of detached particles on Al plate around the bubble. (c) Wide cleaning area due to a traveling bubble on a Si wafer with line patterns after 30 min of particle-substrate contact.

and thus fall out of the focal depth. The bubble interface is blurred because the microscope is focused at the particles and the bubble has an extremely high vibration frequency (0.95 MHz) compared to the exposure duration for a single image (13 μs). When a bubble oscillates while adhered to the solid surface as in Fig. 4(b), detached particles are seen to circulate around the bubble, although their traces are blurred due to high rotational speed. In both the cases in Figs. 4(a) and 4(b), particles situated farther than approximately one bubble radius from the bubble are disturbed little, indicating short-ranged nature of the force generated by the oscillating bubble. However, the effective cleaning area where particles are affected by an oscillating bubble increases as the particle adhesion gets weaker. Figure 4(c) shows that particles that have been in contact with solid for only 30 min are detached over much wider area than the particles in Fig. 4(a), which have sat on solid for 3 h. More visual evidences of megasonic bubbles detaching particles from substrates can be viewed in supplemental videos available online.[11]

We propose that particles near radially oscillating bubbles can be detached from a solid surface by two mechanisms. Liquid-gas interface is passed through by a particle sitting within the oscillation range during the bubble's radial motion. Then the torque due to the Laplace pressure, $\Delta p_L = 2\sigma/R_b$, where σ is the surface tension and R_b is the bubble radius, is exerted on the particle. Multiplying Δp_L, the projection area of the particle A_p and the moment arm give the detachment torque due to interface sweeping, $\tau_i \sim 2\pi R^3\sigma/R_b$. On the other hand, particles sitting outside the range swept by the meniscus are affected by the pressure gradient $|\partial p/\partial r|$, where $p \sim \frac{1}{2}\rho v^2$, the velocity $v \sim \omega R_b(R_b/r)^2$, and r is the radial distance from the bubble center. Then the torque due to the dynamic pressure gradient is scaled as $\tau_d \sim (8\pi/3)\rho\omega^2 R^4 R_b^6/r^5$, which decays with r^{-5} showing indeed its short-ranged nature. As shown in Fig. 2, τ_i is sufficiently strong to detach particles, and the magnitude of τ_d is comparable to the adhesion torque only when particles are fairly close to the bubble, which agrees with our experimental observations.

In summary, the movies obtained through this work reveal that megasonic cleaning is achieved by local fluid motion induced by oscillating bubbles close to resonant size. The estimation of the exerted torque by the two proposed mechanisms provides a possible explanation. Globally generated acoustic pressure gradient and acoustic streaming have little direct effects on the particle removal. However, we point out that they may play secondhand roles in cleaning. For the cleaning of an entire wafer, multiple bubbles should move around so that their paths can cover the entire surface. This bubble movement is primarily caused by Bjerknes force, which is the result of the acoustic pressure gradient. Furthermore, the particles lifted off the solid surface must be driven away to prevent reattachment, which could be made possible by acoustic streaming. It is also worth noting that the mechanism of megasonic cleaning is different from that of the surface cleaning by millimeter-sized bubbles (that can be generated by laser irradiation[13]), which collapse to generate a high-speed liquid jet onto a solid surface.

This work was supported by Samsung Electronics and KRF (Grant No. KRF-2007-412-J03001) and administered by SNU Engineering Research Institute.

[1] M. O. Lamminen, H. W. Walker, and L. K. Weavers, J. Membr. Sci. **237**, 213 (2004).
[2] H. Kuttruff, *Ultrasonics Fundamentals and Applications* (Elsevier, London, 1991).
[3] W. L. Nyborg, *Nonlinear Acoustics* (Academic, New York, 1998), p. 207.
[4] A. A. Doinikov, Phys. Fluids **14**, 1420 (2002).
[5] M. Olim, J. Electrochem. Soc. **144**, 3657 (1997).
[6] K. Bakhtari, R. O. Guldiken, P. Makaram, A. A. Busnaina, and J. Park, J. Electrochem. Soc. **153**, G846 (2006).
[7] T. Ohmi, M. Toda, M. Katoh, K. Kawada, and H. Morita, Mater. Res. Soc. Symp. Proc. **477**, 3 (1997).
[8] F. Zhang, A. A. Busnaina, M. A. Fury, and S. Wang, J. Electron. Mater. **29**, 199 (2000).
[9] H. Krupp, *Particle Adhesion: Theory and Experiment* (Elsevier, New York, 1967), Vol. 1.
[10] B. Niemczewski, Ultrason. Sonochem. **14**, 13 (2007).
[11] See EPAPS Document No. E-APPLAB-94-051909 for high-speed movies showing megasonic bubbles detaching particles from substrates. For more information on EPAPS, see http://www.aip.org/pubservs/epaps.html.
[12] P. Marmottant and S. Hilgenfeldt, Nature (London) **423**, 153 (2003).
[13] C. D. Ohl, M. Arora, R. Dijkink, V. Janve, and D. Lohse, Appl. Phys. Lett. **89**, 074102 (2006).